Increasing the Interlayer Bond of Fused Filament Fabrication Samples with Solid Cross-Sections using Z-Pinning

Chad Duty[1,2], Tyler Smith[1,2], Alexander Lambert[1,2], Justin Condon[1,2],
John Lindahl[2], Seokpum Kim[1,2], Vlastimil Kunc[1,2,3]

[1]University of Tennessee
[2]Manufacturing Demonstration Facility, Oak Ridge National Laboratory
[3]Purdue University

Abstract

The mechanical properties of parts made by fused filament fabrication is highly anisotropic, with the strength across layers (z-axis) typically measuring ~50% lower than the strength along the direction of the extruded material (x-axis). A z-pinning method has been developed in which material is extruded in the z-direction to fill intentionally aligned voids in the x-y print pattern. In previous studies that involved a sparse rectilinear grid cross-section (35% infill), the z-pinning approach demonstrated more than a 3.5x increase in strength in the z-direction. The current study expanded these efforts to evaluate the use of z-pins in a printed sample with a solid cross-section. Although a solid cross-section is more common in structural components, it is much less forgiving of instabilities that may occur in the z-pinning approach (such as over-filling). Even though this study utilized a low pin volume (~43% fill factor), the pinning approach demonstrated a 40% increase in z-direction strength for solid samples that had similar printing times.

Introduction

Material extrusion (MatEx) printing techniques deposit successive layers of material in the x-y plane to create three-dimensional objects. For a simple 0/0 infill pattern, individual layers are comprised of long beads of continuous material (x-direction) that are a placed adjacent to one another in the y-direction. Various infill patterns are used to balance mechanical properties in the x-y plane, the most common of which are a 0/90 or a 45/-45 configuration in which the primary deposition direction rotates 90 degrees from the previously deposited layer. Regardless of the infill pattern, the layer-wise deposition results in relatively continuous material in the x-y plane, but discontinuous material in the z-direction (across layers). Transmitting a tensile load in the z-direction relies on the strength of intermittent bonds between overlapping sections of deposited beads in successive layers.

The discontinuous nature of MatEx structures leads to a significant level of mechanical anisotropy. A number of studies have shown that the tensile strength of parts produced on small scale printers with common materials, such as acrylonitrile butadiene styrene (ABS) and polylactic acid (PLA), is reduced by 50% to 80% in the z-direction [1-3]. The addition of reinforcing fibers to the polymer matrix increases the degree of mechanical anisotropy on both small- and large-scale platforms [1, 2, 4, 5].

Various approaches have attempted to reduce the mechanical anisotropy of MatEx components. The majority of efforts improve the interlayer bond strength by controlling the temperature between layers to encourage molecular diffusion and increased entanglement. Localized heating of the bond interface during the printing process using forced air [6], laser irradiation [7, 8], and infrared lamps [9] have each demonstrated improved performance. Post-processing techniques have also attempted to improve bond strength of MatEx parts by exposing the component to ionizing radiation [3], microwave energy [10], or elevated temperatures [11]. Other researchers are exploring techniques to print out-of-plane to either align the strong direction of the structure with the primary load direction [12, 13] or print a secondary structure around the periphery of the part to reinforce the layered core [13, 14].

The current research investigates the effectiveness of a z-pinning approach for MatEx printing, which deposits continuous material across layers throughout the bulk of a part by extruding into intentionally aligned voids. The patent-pending z-pinning approach that was introduced in 2017 [15, 16] is illustrated in Figure 1. As the primary structure (white) is being printed, voids (diameter, D_H) are positioned such that they align in the z-direction. In the example of Figure 1, the first two layers of the primary structure are printed with voids (a) and (b) remaining. Between deposition of the second and third layers, the print head is positioned over void (a) and material is extruded while the print head is stationary, filling void (a). The second void (b) remains unfilled until layers three and four are printed along with the first two layers of void (c). After layer four is complete, the print head is held stationary over void (b) and material is extruded to fill the void

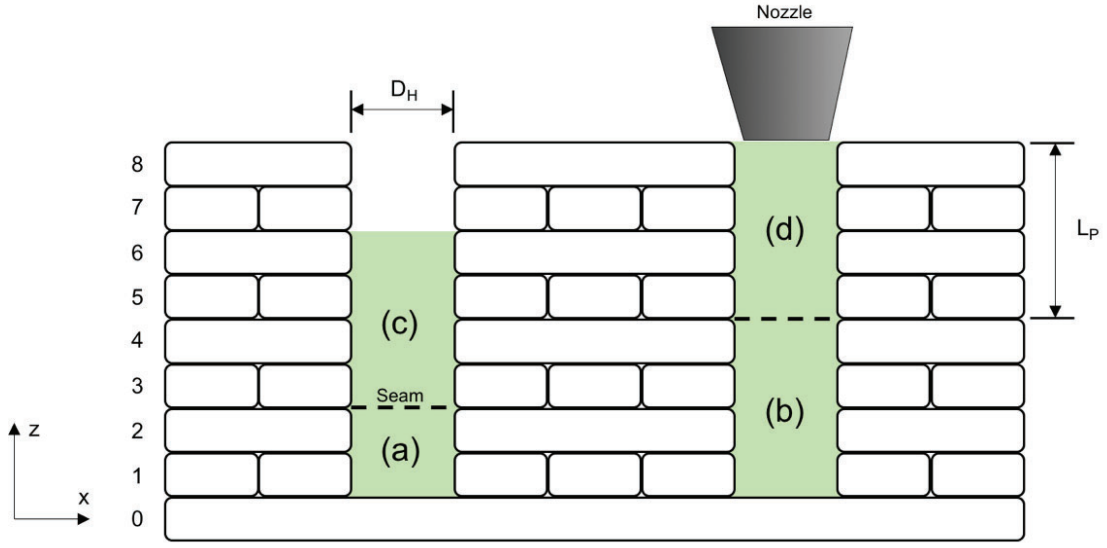

Figure 1. Schematic of the z-pinning process.

(note that the first two layers of void (c) remain open). After layers five and six are deposited, the pinning process is repeated to fill void (c), leaving a seam between pins (a) and (c). A similar seam exists between layers four and five at the interface between pins (b) and (d). Note that the seam positions are staggered due to the alternating pin positions.

The pinning pattern can be extended throughout the bulk of the printed component in all directions. In the example of Figure 1, the standard pin length (L_P) is four layers and pins are extruded into alternating holes every two layers. The labeling convention for this type of configuration is a "4-2 pin". The theoretical volume of the void can be calculated from the void diameter (D_H) and length (L_P). The extruded volume of the corresponding pin to fill the void can range from a small percentage of this theoretical volume to well over 100%, depending on the surrounding structure. In an earlier study [17], sparse rectilinear structures were investigated that had an open architecture, allowing fill factors (pin volume / void volume) to reach 120%. The ultimate tensile strength in the x-direction (UTS_X) and z-direction (UTS_Z) are compared in Figure 2 for carbon fiber reinforced PLA (CF-PLA) structures evaluated during that study. The solid structure was a dense rectilinear grid pattern with no pins, which demonstrated an expected anisotropy of ~33%. The sparse rectilinear grid sample spaced the adjacent beads to create an open architecture with a 35% infill. The sparse structure without pins was much weaker than the solid structure (80-90% drop) and it demonstrated an even higher degree of mechanical anisotropy (~63%). When 8-4 pins were added to the sparse structure, the UTS_Z more than tripled and the mechanical anisotropy was cut in half.

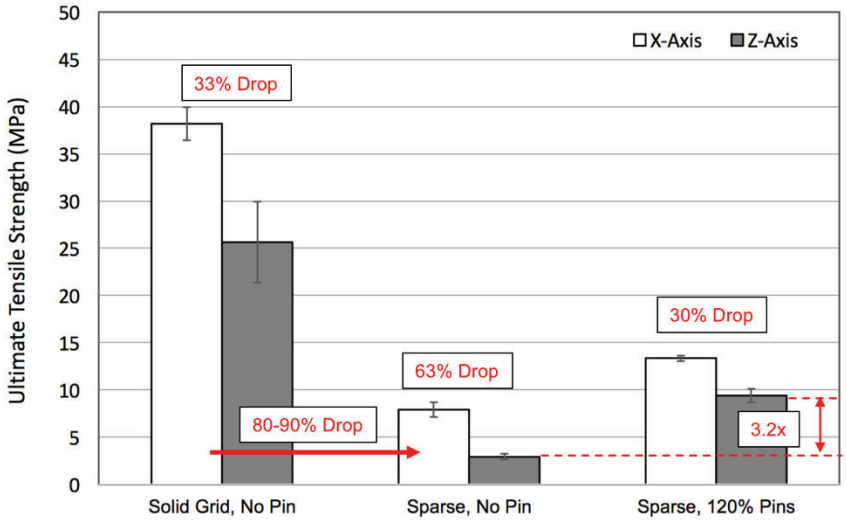

Figure 2. Average ultimate tensile strength of CF-PLA printed samples.

The current study extends the z-pinning technique to more conventional solid structures that have a 45/-45 infill pattern [18]. Placing z-pins into a solid structure is much more difficult due to the lack of interstitial space for the pin to expand into. Due to the layered nature of a MatEx structure, the internal walls of the voids are inherently rough (scalloped – see Figure 1), so the pin can still partially mechanically interlock with the surrounding structure. However, since the solid structure is less forgiving of print variations, it is difficult to achieve fill factors that approach 100%.

Experimental Methods

The material used for this study was a 15% carbon fiber reinforced PLA (CF-PLA) purchased as CarbonX from 3DXTech. Samples were produced on a MakerGear M2 desktop printer with a print temperature of 245ºC. The individual tensile samples were harvested from a single vertical wall, measuring 127 mm (x) x 12.7 mm (y) x 127 mm (z). The dimensions of the tensile sample are shown in Figure 3 as they are waterjet cut from the printed vertical wall. The samples were dried in an oven at 50ºC for at least 8 hours and stored in a desiccant chamber prior to tensile testing on an MTS servo-hydraulic test system (110 kN load cell, strain rate of 3 mm/min).

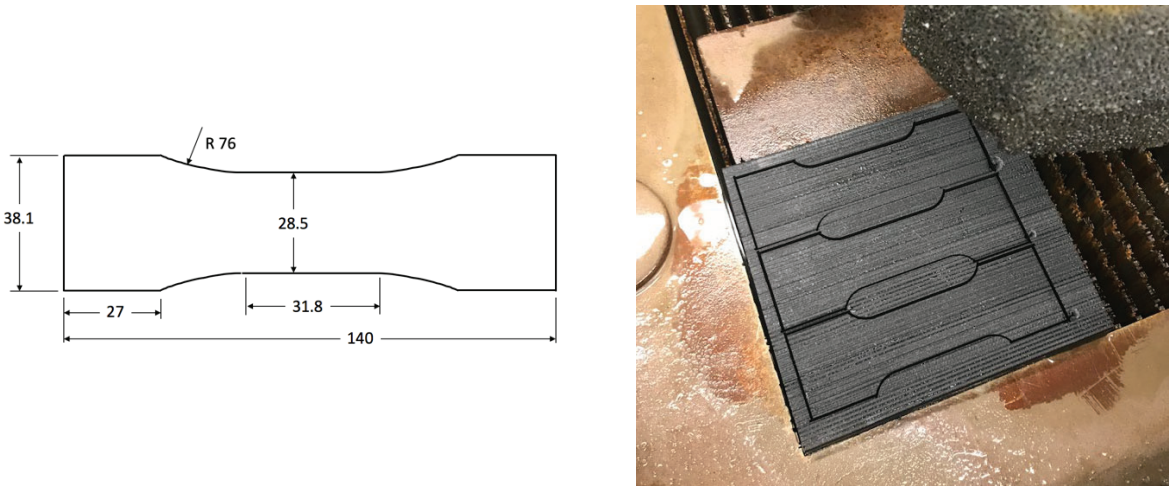

Figure 3. Tensile sample dimensions (left) in mm waterjet cut from printed wall (right).

A conventional solid sample with 45/-45 infill pattern was printed as an initial control reference. As shown in Figure 4, the print time for the solid sample included only sum of the times to print the individual layers (No Pin, No Pause). When pins were added on every fourth layer (8-4 Pins), it consumed an additional 55 seconds each time, increasing the print time of that particular layer by more than 50%. Since the strength of the interlayer bond has been attributed to maintaining a high interfacial temperature [19-21], the additional time during every fourth layer could significantly cool the interface and weaken the structure. Therefore, a more appropriate control sample was also printed without pins that included a pause on every forth layer to match the print time of the pinned samples (No Pin w/ Pause). In practice, this could be representative of a much larger part that would naturally have longer layer times.

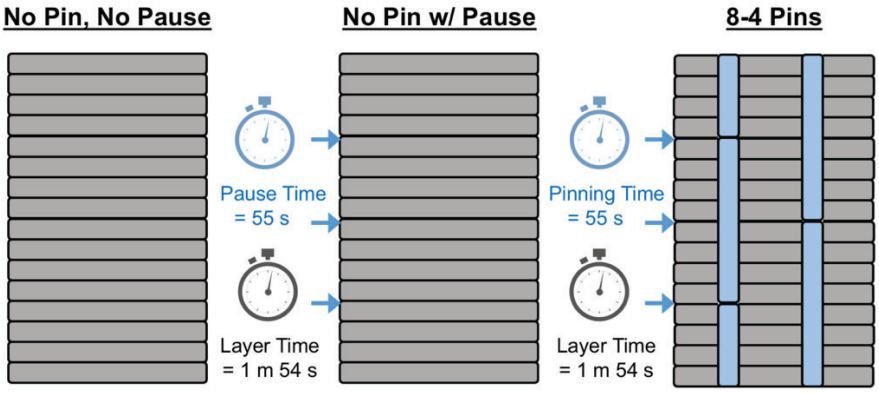

Figure 4. Print time comparison among solid samples.

Two pinning configurations were considered for this study. Both sample sets utilized three rows of 8-4 pins across the thickness of the sample with a fill factor of 43%. The pinning configuration within the x-y plane was varied among the two sample sets as shown in Figure 5. For this figure, consider that the "K^{th}" pin in the "A" location would be deposited after layer (Kn) while the K^{th} pin in the "B" locations would be deposited after layer (Kn+m), where pins of length (n) are inserted every other (m) layers. For the example of the 4-2 pins (n=4, m=2) in Figure 1, pin (b) would be the first "A" pin (K=1) deposited after layer 4, and pin (c) would be the first "B" pin (K=1) deposited after layer 6. When (n/2 = m), the seams between "A" pins are located on the same layer as the mid-point of the "B" pins. Figure 5 shows a "Standard" pinning configuration where the "A" pins are located on alternating rows of the x-y plane. If a fracture occurred across a given x-y plane, the Standard configuration involving only three rows of pins would be unevenly balanced. The "Staggered" configuration alternates the pin locations along a given row, providing more balance across a 3 row structure.

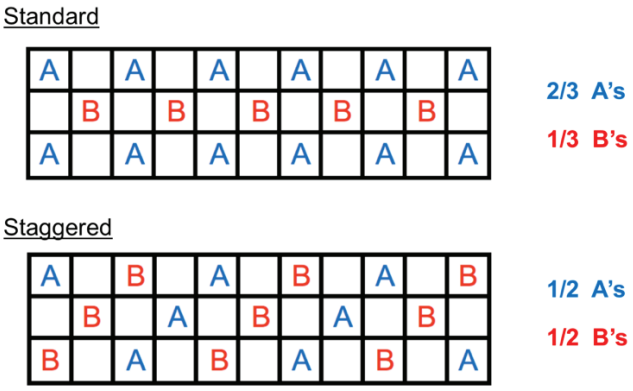

Figure 5. Comparison of pin spacing patterns in the x-y plane.

Results and Discussion

The ultimate tensile strength in the z-direction of the printed samples are shown Figure 6. The conventional solid sample that was printed without pauses is clearly the best performing structure, with a UTS_Z of 33 MPa. When the same structure was printed with a 55 second pause on every fourth layer, the strength dropped to a baseline value of 12 MPa (64% reduction). The addition of z-pins to the structure improved the UTS_Z by roughly 40% regardless of the pinning configuration used (Standard = 17 MPa, Staggered = 16 MPa). Although the strength of the pinned structure did not approach the solid sample printed without pausing, this represents a significant improvement in strength when compared to parts that may be cooling down considerably between successive layers (e.g. a large part with a naturally long layer time).

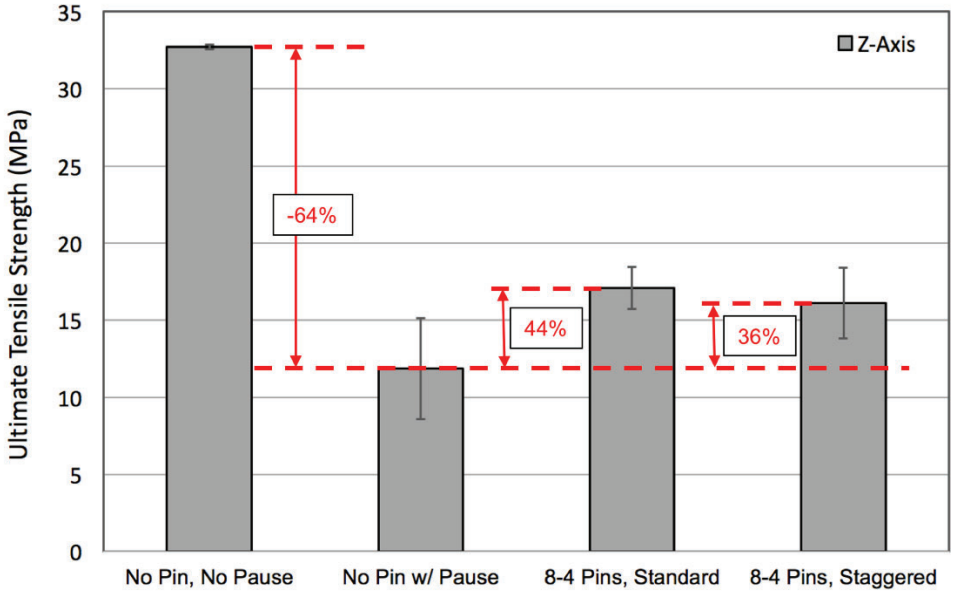

Figure 6. Average ultimate tensile strength of solid printed samples (CF-PLA).

The fracture surfaces of the tensile samples are shown in Figure 7. It is apparent that the unpinned sample had a very clean fracture surface, with the crack front progressing unobstructed across the layer-to-layer interface (note: the two unpinned sample sets looked very similar). In contrast, the two pinned samples resulted in very tortuous fracture surfaces as the crack front deflected around the solid pins to find the weaker interfaces at the seams. The pin locations for the latter two samples are highlighted in Figure 8, along with a schematic of the observed crack front progression in the z-direction. It appears that the crack front crossed the pin locations at the seams between pins rather than fracturing the pin or pulling it out of the structure. Close inspection of Figure 8a shows a "string" of material originating from the red pin locations and stretching out in a line (left-to-right) toward the next pin location. This is an artifact of a non-optimized pinning process, where the extruded pin has slightly overfilled the hole and excess material has been dragged along the surface to the next pin location. A similar pattern can be seen in the lower row of blue pins in Figure 8a, but this time apparently originating on the right-most pin and being dragged to the left.

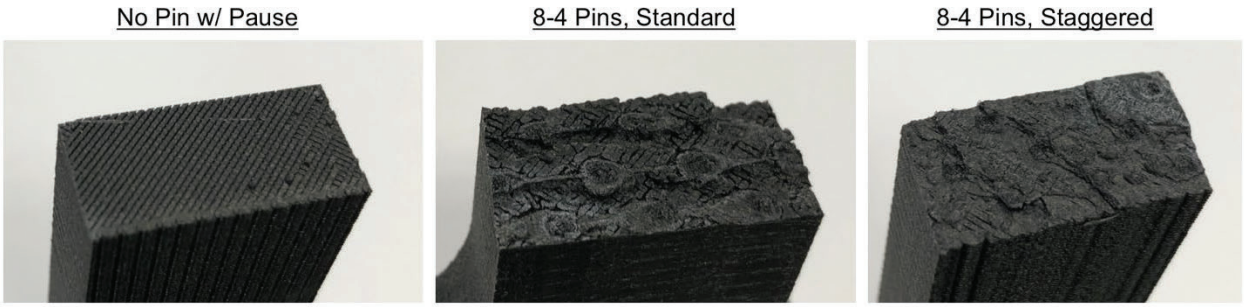

Figure 7. Representative fracture surfaces of tensile samples (CF-PLA).

A "stair-stepping" effect was observed at the fracture surface, but it is not readily apparent in the photographs in Figures 8a and 8c. The seams in the Standard pin configuration remained constant within a given row. Near bottom of the sample in Figure 8a, each of pins colored blue have a seam at the same layer height, which is 4 layers below the seam locations of the middle row of pins colored red. Observing the fractured sample from the side (schematically illustrated in Figure 8b) showed that the crack front distinctly shifted across the width of the sample to cross at the new seam location. As the crack progressed to the third row (blue pins), the fracture surface shifted up a similar amount to cross the seams of the two pins on the left, but actually shifted back down to the original layer height to cross the lower seam of the pin in the back right (dashed line in Figure 8b). A similar stair-stepping effect was observed in the Staggered sample in Figure 8c. In this configuration, the seam locations are at the same height for pins that are diagonally positioned. So rather than progressing across rows, the stair-step path progressed diagonally across the sample, continuing to gain height when moving from left-to-right (positive x-direction) in Figures 8c and 8d. The color-coded sections in Figure 8d illustrate the height of the fracture surface that is aligned with the seam of a given pin. These fracture patterns indicate that the weakest location under the current printing conditions is the seam between adjacent pins, which could result from under-filling of voids. Future work will investigate alternate configurations and optimize print conditions.

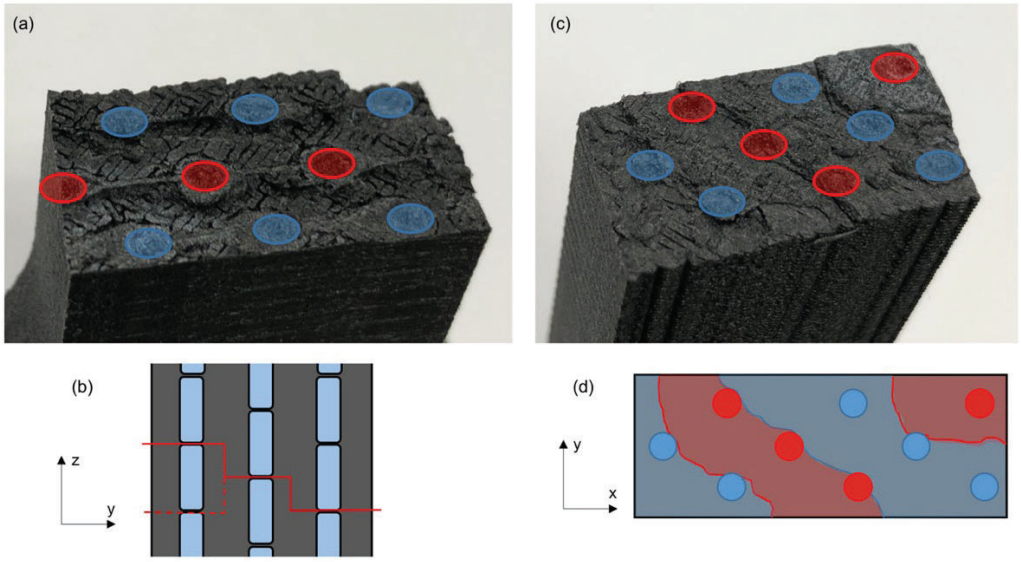

Figure 8. Fracture surface analysis relative to pin position.

Conclusions and Future Work

The z-pinning approach has been demonstrated for MatEx samples with a solid cross section. The strength of solid samples without pins was found to be very sensitive to the layer time; less than a one minute delay on every fourth layer caused the UTS_Z to decrease by more than 60%. The addition of z-pins to the structure was able to increase the z-strength by ~40% regardless of the pinning configuration used. Inspection of the fracture surface of pinned samples revealed that the crack front navigated to the seams between adjacent pins, indicating that defects may be present due to incomplete filling of the void intended for the pin. Because solid samples do not have an open architecture, the placement and extrusion of pins is less forgiving than sparse structures and additional optimization of the printing process and pin geometry is required.

Acknowledgements

Research sponsored by the U.S. Department of Energy, Office of Energy Efficiency and Renewable Energy, Industrial Technologies Program, under contract DE-AC05-00OR22725 with UT-Battelle, LLC.

References

[1] Torrado-Perez, A., D. Roberson, and R. Wicker. (2014) "Fracture Surface Analysis of 3d-Printed Tensile Specimens of Novel Abs-Based Materials". *Journal of Failure Analysis and Prevention* **14** pp. 343-353.

[2] Torrado, A.R., C.M. Shemelya, J.D. English, Y. Lin, R.B. Wicker, and D.A. Roberson. (2015) "Characterizing the Effect of Additives to Abs on the Mechanical Property Anisotropy of Specimens Fabricated by Material Extrusion 3d Printing". *Additive Manufacturing* **6** pp. 16-29.

[3] Shaffer, S., K. Yang, J. Vargas, M. Di-Prima, and W. Voit. (2014) "On Reducing Anisotropy in 3d Printed Polymers Via Ionizing Radiation". *Polymer* **55** pp. 5969-5979.

[4] Duty, C.E., V. Kunc, B. Compton, B. Post, D. Erdman, R. Smith, R. Lind, P. Lloyd, and L. Love. (2017) "Structure and Mechanical Behavior of Big Area Additive Manufacturing (Baam) Materials". *Rapid Prototyping Journal* **23** (1).

[5] Zhong, W., F. Li, Z. Zhang, L. Song, and Z. Li. (2001) "Short Fiber Reinforced Composites for Fused Deposition Modeling". *Materials Science and Engineering: A* **301** (2) pp. 125-130.

[6] Partain, S., *Fused Deposition Modeling with Localized Pre-Deposition Heating Using Forced Air*. 2007, Montana State University.

[7] Ravi, A., *A Study on an in-Process Laser Localized Pre-Deposition Heating Approach to Reducing Fdm Part Anisotropy*. 2016, Arizona State University.

[8] Ravi, A., A. Deshpande, and K. Hsu. An in-Process Laser Localized Pre-Deposition Heating Approach to Inter-Layer Bond Strengthening in Extrusion Based Polymer Additive Manufacturing. 2016.

[9] Kishore, V., C. Ajinjeru, A. Nycz, B. Post, J. Lindahl, V. Kunc, and C. Duty. (2016) "Infrared Preheating to Improve Interlayer Strength of Big Area Additive Manufacturing (Baam) Components". *Additive Manufacturing* **14** pp. 4-12.

[10] Sweeney, C.B., B.A. Lackey, M.J. Pospisil, T.C. Achee, V.K. Hicks, A.G. Moran, B.R. Teipel, M.A. Saed, and M.J. Green. (2017) "Welding of 3d-Printed Carbon Nanotube–Polymer Composites by Locally Induced Microwave Heating". *Science Advances* **3** (6).

[11] Kishore, V., X. Chen, A. Hassen, J. Lindahl, V. Kunc, and C. Duty. (2019) "Effect of Post-Processing Annealing on Crystallinity Development and Mechanical Properties of Polyphenylene Sulfide Composites Printed on Large-Format Extrusion Deposition System" *SAMPE Conference & Exhibition.* Charlotte, NC. May 20-23, 2019

[12] Khurana, J., T.W. Simpson, and M. Frecker. Structurally Intelligent 3d Layer Generation for Active Z-Printing." in Solid Freeform Fabrication Symposium. 2018. Austin, TX.

[13] Kubalak, J., C. Mansfield, T. Pesek, Z. Snow, E. Cottiss, O. Ebeling-Koning, M. Price, M. Traverso, L. Tichnell, C.B. Williams, and A. Wicks. Design and Realization of a 6 Degree of Freedom Robotic Extrusion Platform." in Solid Freeform Fabricatin Symposium. 2016. Austin, TX.

[14] Kubalak, J.R., A.L. Wicks, and C.B. Williams. (2018) "Using Multi-Axis Material Extrusion to Improve Mechanical Properties through Surface Reinforcement". *Virtual and Physical Prototyping* **13** (1) pp. 32-38.

[15] Duty, C., J. Failla, S. Kim, J. Lindahl, B. Post, L. Love, and V. Kunc. (2017) "Reducing Mechanical Anisotropy in Extrusion-Based Printed Parts" *Solid Freeform Fabrication Symposium.* Austin, TX. August 2017

[16] Duty, C., J. Failla, V. Kunc, J. Lindahl, B. Post, L. Love, and S. Kim (2018) "Z Layer Improvement Using Liquid Nails Method." U.P. Application 15/965,106 filed April 27, 2018.

[17] Duty, C., J. Failla, S. Kim, T. Smith, J. Lindahl, and V. Kunc. (2019) "Z-Pinning Approach for 3d Printing Mechanically Isotropic Materials". *Additive Manufacturing* **27** pp. 175-184.

[18] Duty, C., J. Failla, S. Kim, T. Smith, J. Lindahl, A. Lambert, and V. Kunc. (2019) "Z-Pinning Approach for Improving Interlaminar Strength of 3d Printed Parts" *SAME Conference & Exhibition.* Charlotte, NC. May 20-23, 2019

[19] Rodriguez, J.F., J.P. Thomas, and J.E. Renaud. (2003) "Mechanical Behavior of Acrylonitrile Butadiene Styrene Fused Deposition Materials Modeling". *Rapid Prototyping Journal* **9** (4) pp. 219-230.

[20] Sun, Q., G.M. Rizvi, C.T. Bellehumeur, and P. Gu. (2008) "Effect of Processing Conditions on the Bonding Quality of Fdm Polymer Filaments". *Rapid Prototyping Journal* **14** (2) pp. 72-80.

[21] Turner, B., R. Strong, and S. Gold. (2014) "A Review of Melt Extrusion Additive Manufacturing Processes: I. Process Design and Modeling". *Rapid Prototyping Journal* **20** (3) pp. 192-204.